

let-7g-5p Suppresses the Proliferation and Expansion of Hepatic Stellate Cells in Liver Fibrosis via Targeting FGF5

(let-7g-5p Mencegah Proliferasi dan Pengembangan Sel Stellate Hepatik dalam Fibrosis Hati melalui Penyasaran FGF5)

JIAMING ZHOU^{1,2,3†*}, SIYAN HUANG^{1,2†}, YIDAN YANG^{1,2}, YUTONG CONG², YUWEN CHEN², YOUYOU DING², MENGWEN LU², MEIYUAN LI^{1,2}

¹Department of Pathology, Medical School of Nantong University, Nantong 226001, Jiangsu, China

²Department of Medicine, Xinglin College of Nantong University, Nantong 226001, Jiangsu, China

³Department of Pathology, Second Affiliated Hospital of Naval Medical University, Shanghai 200003, China

Received: 28 April 2024/Accepted: 13 December 2024

†Jiaming Zhou and Siyan Huang contributed equally to this work

ABSTRACT

Hepatic stellate cells (HSCs) and their activated phenotype (activated HSCs, aHSCs) function as crucial effector cells in the onset of liver fibrosis. In recent years, microRNAs (miRNAs) have emerged as a promising therapeutic approach for diseases. To explore early intervention strategies for HSCs activation and proliferation, miRNA profiles were sequenced from three patients with chronic hepatitis B-related hepatic fibrosis (HF). The miRNAs sequencing experiment and data analysis were conducted utilizing the Illumina HiSeq 4000 platform. *In vitro*, the proliferation and expansion capabilities of HSCs were detected using CCK8, EdU and colony formation assays. The examination of α -SMA, the indicator aHSCs, was performed through western blot assays. For *in vivo* investigation of the let-7g-5p/FGF5 axis, a bile duct ligation (BDL)-induced HF mice model was constructed and mmu-let-7g-5p agomir was delivered to mice via tail vein injection. Collagen deposition and the α -SMA level were assessed through histological staining including H&E, Masson, Van Gieson (VG), and immunohistochemical (IHC) staining. The miRNAs sequencing and bioinformatics analysis identified let-7g-5p as a promising anti-HF candidate. qRT-PCR and dual-luciferase reporter assays confirmed FGF5 as the direct target of let-7g-5p. let-7g-5p hampered the proliferation and expansion abilities of HSCs and decreased the α -SMA level by targeting FGF5 *in vitro*. In addition, H&E, Masson, VG and IHC staining demonstrated the let-7g-5p/FGF5 axis significantly mitigated collagen deposition and decreased α -SMA production in the BDL-induced HF mice. let-7g-5p suppressed the proliferation and expansion of HSCs and alleviated HF via targeting FGF5. The let-7g-5p/FGF5 axis could be an effective therapeutic target for reducing aHSCs abundance in HF.

Keywords: Bile duct ligation; FGF5; hepatic fibrosis; hepatic stellate cells; let-7g-5p; proliferation; α -SMA

ABSTRAK

Sel bintang hepatic (HSC) dan fenotip yang diaktifkan (HSC diaktifkan, aHSC) berfungsi sebagai sel efektor penting dalam permulaan fibrosis hati. Dalam beberapa tahun kebelakangan ini, mikroRNA (miRNA) telah muncul sebagai pendekatan terapeutik yang berpotensi untuk penyakit. Untuk meneroka strategi intervensi awal untuk pengaktifan dan percambahan HSC, profil miRNA telah diujikan daripada tiga pesakit dengan fibrosis hepatic (HF) berkaitan hepatitis B kronik. Uji kaji penjujukan miRNA dan analisis data telah dijalankan menggunakan platform Illumina HiSeq 4000. Secara *in vitro*, keupayaan percambahan dan pengembangan HSC telah dikesan menggunakan CCK8, EdU dan ujian pembentukan koloni. Pemeriksaan α -SMA, penunjuk aHSC, telah dilakukan melalui ujian pemblokan western. Untuk kajian *in vivo* paksi let-7g-5p/FGF5, model tikus HF yang disebabkan oleh pengikatan saluran hempedu (BDL) telah dibina dan mmu-let-7g-5p agomir dihantar kepada tikus melalui suntikan urat ekor. Pemendapan kolagen dan tahap α -SMA dinilai melalui pewarnaan histologi termasuk pewarnaan H&E, Masson, Van Gieson (VG) dan pewarnaan imunohistokimia (IHC). Penjujukan miRNA dan analisis bioinformatik mengenal pasti let-7g-5p sebagai calon anti-HF yang berpotensi. Ujian reporter qRT-PCR dan dwi-luciferase mengesahkan FGF5 sebagai sasaran langsung let-7g-5p. let-7g-5p menghalang kebolehan percambahan dan pengembangan HSC dan mengurangkan tahap α -SMA dengan menyasarkan FGF5 secara *in vitro*. Di samping itu, pewarnaan H&E, Masson, VG dan IHC menunjukkan paksi let-7g-5p/FGF5 dengan ketara mengurangkan pemendapan kolagen dan mengurangkan pengeluaran α -SMA pada tikus HF yang disebabkan oleh BDL. let-7g-5p menyekat percambahan

dan pengembangan HSC dan mengurangi HF melalui menyasarkan FGF5. Paksi let-7g-5p/FGF5 boleh menjadi sasaran terapeutik yang berkesan untuk mengurangkan kelimpahan aHSC dalam HF.

Kata kunci: FGF5; fibrosis hepatic; let-7g-5p; ligasi saluran hempedu; percambahan; sel bintang hepatic; α -SMA

INTRODUCTION

Hepatic fibrosis (HF) is a complex response produced in the process of long-term liver damage (Li et al. 2023; Wang et al. 2019). In healthy livers, hepatic stellate cells (HSCs), which reside in the space of Disse (Thanh et al. 2021), are quiescent and store vitamin A within their intracellular lipid droplets. In cases of liver injury, HSCs experience a reduction in vitamin A levels and undergo transdifferentiation into a myofibroblast (MF)-like phenotype, which are commonly known as activated HSCs (aHSCs). These aHSCs produce α -smooth muscle actin (α -SMA), obtain robust contractile and proliferative capabilities and secrete large amounts of extracellular matrix (ECM) (Geerts et al. 2001; Pei, Yi & Tang 2023). This process leads to the aberrant accumulation of collagen, disrupts the normal hepatic architecture, and initiates the fibrosis in liver.

In recent years, some advancements have been achieved in the early intervention of HF. Two studies showed that treatment with pirfenidone and benzoisidone partially reversed fibrosis and restored normal liver architecture in rodent HF models induced by carbon tetrachloride (CCl₄) and bile duct ligation (BDL) (García et al. 2002; Wasser et al. 2001). In addition, Wanless, Nakashima and Sherman (2000) demonstrated that lamivudine treatment in patients with chronic hepatitis B significantly alleviated the degree of liver fibrosis. Friedman (2015), a renowned hepatology expert, has identified the primary strategies for reversing HF as follows: (1) controlling the pathogenesis; (2) reducing liver damage; (3) inhibiting the activation of myofibroblasts (MFB); (4) stimulating matrix degradation; and (5) promoting apoptosis or facilitating the reversion of aHSCs. Suppressing aHSCs is considered the most promising therapeutic approach for the early intervention of HF.

The regulatory role of endogenous microRNAs (miRNAs) in organ fibrosis has recently attracted much attention (Wang et al. 2020; Yao et al. 2018). Through targeting TGFBR2, miR-7 modulated the epithelial-mesenchymal transition process during pulmonary fibrosis (Yao et al. 2018). miR-122 suppressed the HSCs activation via targeting TGF- β 1 (Cheng et al. 2019). miR-708/TMEM88 axis enhanced the ECM accumulation in liver via the WNT/ β -catenin signaling pathway (Xu et al. 2020). Hepatitis B Virus (HBV) infection is one of the most common causes of HF (Chien et al. 2020—; Wei et al. 2018). HBV infection is particularly prevalent in China and southeastern Asia, leading to immense potential treatment audience for HF in these areas (Ho, Jeevan-Raj & Netter 2020). To develop a universal intervention strategy, we collected three hepatitis B-related HF samples for RNA

sequencing (RNA-seq) and obtained the human HF miRNA profile.

Through bioinformatics analysis, the study primarily identified let-7g-5p as a potential candidate for anti-HF therapy, and demonstrated fibroblast growth factor 5 (FGF5) as the direct target gene of let-7g-5p. This study aims to elucidate how the let-7g-5p/FGF5 axis affects the proliferation and expansion of HSCs *in vitro* and *in vivo*. The findings are anticipated to be beneficial in identifying molecular targets for inhibiting the proliferation of HSCs and reducing the abundance of aHSCs.

MATERIALS AND METHODS

PATIENTS

This study included thirty-eight patients with chronic hepatitis B-related HF from the Second Affiliated Hospital of Naval Medical University, Shanghai, China. Three patients were used for RNA-seq and additional thirty-five patients were used for further qRT-PCR detection. HF tissues were evaluated by two senior pathologists before inclusion. In Shanghai, China, the Research Ethics Committee of Naval Medical University approved the research. Every participant provided written informed consent to partake in the research. All procedures performed in studies involving human and animals participants were in accordance with the ethical standards of the Ethics Committee of Naval Medical University, Shanghai, China Nantong University, Jiangsu Province, China (Grant No. P20230224-017). The study is reported in accordance with ARRIVE guidelines (<https://arriveguidelines.org>).

RNA-seq ARRAY AND BIOINFORMATICS ANALYSIS

The total RNA of the three hepatitis B-related HF samples was extracted using Trizol Reagent and sent for RNA-seq detection. The RNA-seq experiment and subsequent data analysis were conducted utilizing the Illumina HiSeq 4000 platform. The miRNA sequencing data is uploaded to the supplementary materials. The miRNA data of normal liver tissues were obtained from an NCBI GEO database (<https://www.ncbi.nlm.nih.gov/geo/query/acc.cgi?acc=GSE87843>). The Targetscan, NCBI and DAVID databases were used for target gene prediction and annotation.

CELL CULTURE AND SIRNA/MIMICS/INHIBITORS TRANSFECTION

LX-2, an immortalized human HSC cell line, was routinely cultured in DMEM medium supplemented with 100 units/

mL penicillin and 10% fetal bovine serum (Gibco, USA). The LX-2 cells were transfected with siRNA/mimics/inhibitors using lipofectamine 2000 (Invitrogen, CA, USA). Taking six-well transfection as an example, siRNA/mimics/inhibitors 75 pmol was diluted in 100 μ L Opti-MEM® I Medium (Life Technologies) and mixed gently. Then, lipofectamine 2000 7.5 μ L was diluted in another 100 μ L Opti-MEM® I Medium. The two liquids mentioned above were mixed to form the transfection complex. After incubating at room temperature for 15 min, the reaction mixture was added to a 6-well plate. Transfected cells were harvested and used for subsequent experiments 48 h later. siRNA targeting FGF5 used in this study was designed and synthesized by Shanghai Saideng Biotechnology Company, including siRNA-1: s CACGGUACUGUCCUGAAAdTdT, As UUCAGGAACAGUAACCGUGdTdT; siRNA-2: s GCAAUACAUAAGAACUGAAAdTdT, As UUUCAGUUCUAUGUAUUGCdTdT; and siRNA-3: s GUUUCCAUCUGCAGAUCUAdTdT, As UAGAUCUGCAGAUGGAAACdTdT. miRNA products were purchased from Ruibo Bio (Guangzhou, China).

QUANTITATIVE RT-PCR (qRT-PCR)

Trizol Reagent was used for the extraction of the total RNA of LX-2 cells. A reverse transcription kit and an SYBR® Green PCR Kit (No. K1622, No. F-415XL, ThermoFisher) were used for qRT-PCR detection. Briefly, PCR was performed at 94 °C for 10 min, followed by 40 cycles of 94 °C for 20 s, 55 °C for 20 s, and 72 °C for 20 s. GAPDH or U6 was used as a normalization factor for mRNA or miRNA levels. The primer sequences for qRT-PCR are exhibited in Table 1.

WESTERN BLOT ASSAY

We lysed LX-2 cells in RIPA-PMSF (100:1) buffer 48 h after transfection. Polyacrylamide gels with 10% SDS were used for the separation of proteins. Afterward, a 2-h transfer of the proteins was carried out at 350 mA on polyvinylidene fluoride membranes (Millipore, CA, USA). The membranes were incubated using rabbit anti-human FGF5 and rabbit anti-human α -SMA antibodies (Abcam, UK) overnight at 4 °C. Membranes were incubated with secondary antibodies for 2 h (goat-anti-rabbit, Biyuntian, China) and exposed to chemiluminescence the following day. A Tannon 3500 imaging system (Tannon, Shanghai, China) was used for the photos. GAPDH was served as an internal control.

DUAL-LUCIFERASE REPORTER ASSAY

The psiCHECK2-reporter vector was employed for the identification of the interaction between let-7g-5p and FGF5. The psiCHECK2-reporter vector was modified by inserting either the wild-type FGF5 3'UTR or its mutant sequences. let-7g-5p mimics or mimics NC were co-transfected into 293T cells using lipofectamine 2000

(Invitrogen, CA, USA), together with FGF5-3'UTR-WT plasmid or FGF5-3'UTR-MT plasmid. Dual-Luciferase Reporter Assay System (Promega, Madison, USA) was used to measure relative luciferase absorbance 48 h after transfection. The data was normalized to Renilla luciferase absorbance values.

CCK8 ASSAY

96-well plates were seeded with 1×10^3 /mL LX-2 cells in each well overnight. Then, siRNA/mimics/inhibitors were transfected into the cells according to the experimental grouping. After transfecting for 48 h, each well was added with 10 μ L CCK8 (Biyuntian, China). At 37 °C, the samples were incubated for 4 h. Absorbance at 450 nm was measured using microplate readers (BioRad, California).

CELL PROLIFERATION EdU EXPERIMENT

According to experimental design, LX-2 cells were transfected with siRNA/mimics/inhibitors. After transfection for 48 h, an EdU kit (Biyuntian, Hangzhou, China) was used for cell proliferation detection. In accordance with the established protocol of the manufacturer, the 2 \times EdU working solution, which had been pre-warmed, was introduced into the cell plate, resulting in a final concentration of 10 mM. The incubation was terminated after 2 h. The cells were washed three times with a washing solution following fixation in 4% paraformaldehyde for 20 min. Cells were visualized and quantified by fluorescence microscope followed by nuclear counterstaining using DAPI.

COLONY FORMATION ASSAY

In accordance with the experimental design, LX-2 cells were transfected with siRNA/mimics/inhibitors and harvested 48 h after transfection. A 6-well plate was prepared with harvested LX-2 cells, which were subsequently cultured until visible clones emerged. Then, the culture was terminated and 4% paraformaldehyde were used to fix the cells. A 0.1% crystal violet staining solution was used to visualize the cells, and the clones were counted directly under a light microscope (low magnification).

BILE DUCT LIGATION (BDL) MICE HF MODEL

CONSTRUCTION AND mmu-Let-7g-5p AGOMIR INJECTION

For BDL model, twenty female C57BL/6 wild-type mice (4 weeks old, 16-20 g) were randomly divided into four groups: control (n=5), BDL/no treatment (n=5), BDL/agomir NC (n=5), and BDL/let-7g-5p agomir (n=5). Control mice (n=5) for BDL mice were littermates subjected to a sham surgery. The other 15 mice received BDL surgery. In brief, under halothane anesthesia and through a midline laparotomy, the extrahepatic common bile duct was double-ligated with 60 silk and sectioned between the ligatures. Incisions in the abdomen were sutured with silk and individual cages were

provided to the mice for recovery. One week after the BDL operation, mice in BDL/agomir NC group or BDL/let-7g-5p agomir group received tail vein injection of agomir NC or mmu-let-7g-5p agomir, respectively (20 nmol agomir dissolved in 200 μ L saline solution, twice a week). mmu-let-7g-5p agomir or agomir NC are chemically modified double-strand stable miRNA mimics, which were purchased by Ruibo Bio (Guangzhou, China). Mice in BDL/no treatment group received saline injection. All BDL mice were sacrificed after 6 times injections. The liver was removed entirely and photographed. A portion of the liver tissue was fixed in paraformaldehyde and embedded in paraffin for histological evaluations. Ethical Committee of Nantong University, Jiangsu Province, China approved all experimental procedures.

H&E/Masson/VG AND IMMUNOHISTOCHEMICAL (IHC) STAINING

Serial sections of mice livers were cut into four- μ m thickness. Histological evaluations were performed on mice liver sections of by H&E/Masson/VG staining using commercially available kits (Biyuntian, China). For IHC staining, routine deparaffinization and rehydration were performed on sections. Afterwards, primary antibodies were used to incubate the sections overnight at 4 $^{\circ}$ C, including anti-FGF5 and anti- α -SMA (Abcam, UK). The slides were incubated in the secondary antibodies for 50 min at room temperature on the second day. Following that, the slides were visualized with diaminobenzidine and hematoxylin and photographed under a microscope (Zeiss, Thornwood, USA). The Image J Software conducted quantitative analysis of the Masson/VG/IHC-positive area in a minimum of five randomly fields for each slice.

STATISTICAL ANALYSIS

Statistical analysis of the data was conducted using GraphPad Prism 8.0. Statistical significance was assessed through the utilization of the student's t-test, while the data were presented as the mean \pm standard deviation (SD) derived from three independent experiments. A statistically significant difference was identified with a *p*-value of 0.05. The asterisks * and ** represent *p*-values less than 0.05 and 0.01, respectively.

RESULTS

LET-7g-5p WAS SIGNIFICANTLY DOWN-REGULATED IN HEPATITIS B-RELATED HF SAMPLES AND DIRECTLY TARGETED FGF5

Sixty-two fully-sequenced and significantly dysregulated (fold change >2 or <0.5, *p*<0.05) miRNAs were screened in human hepatitis B-related HF tissues, among which 47 miRNAs were significantly up-regulated, and 15 miRNAs

were significantly down-regulated (Figure 1(A) & 1(B)). The miRNAs with the highest fold change and most significant *p*-values were documented in Table 2. This study initially focused on let-7g-5p, which exhibited significant down-regulation and a notably low *p*-value. Given that down-regulated miRNAs typically act as suppressors in diseases, let-7g-5p was preliminary identified as a potential anti-HF candidate for further study.

Using Targetscan, NCBI, and DAVID databases, four fibrosis-related genes, TGFBR1, TGFBR3, FGF5, and FGF11, are predicted as targets of let-7g-5p (Figure 1(C)). Of the genes examined, only FGF5 exhibited a significant decrease in expression following transfection with let-7g-5p mimics in LX-2 cells (Figure 1(D)). Furthermore, the substantial negative correlation between let-7g-5p and FGF5 was confirmed in an additional 35 clinical hepatitis B-related HF samples (Figure 1(E)). The interaction between let-7g-5p and FGF5 was validated using a dual-luciferase reporter assay (Figure 1(F)). The group co-transfected with let-7g-5p mimics and FGF5-3'UTR-WT plasmid exhibited a significant reduction in luciferase activity compared to the group co-transfected with mimics NC and FGF5-3'UTR-WT plasmid. However, when comparing the groups transfected with mimics NC+FGF5-3'UTR-MT plasmid and let-7g-5p mimics+FGF5-3'UTR-MT plasmid, it was observed that the latter did not exhibit a statistically significant discrepancy in luciferase activity (Figure 1(G)). These results indicated that FGF5 functioned as the primary target gene downstream of let-7g-5p.

si-FGF5 INHIBITED THE PROLIFERATION AND EXPANSION OF HSCs, AND DECREASED THE POPULATION OF aHSCs

The functionality of FGF5 was first examined in HSCs because miRNA functions often rely on its downstream target genes. The most effective siRNA targeting FGF5, siRNA-3, was selected for utilization in subsequent experiments (Figure 2(A)). CCK8, EdU, and colony formation assays were performed to examine the proliferation and expansion of HSCs. In CCK8 assay, the proliferation ability of HSCs in the si-FGF5 group was significantly hampered (55.24 \pm 6.19%), as compared with the si-NC group (Figure 2(B)). Additionally, the percentage of EdU-positive (EdU/DAPI) HSCs in the si-FGF5 group (16.11 \pm 4.12%) was also inhibited considerably compared with the si-NC group (30.32 \pm 3.59%) (Figure 2(C)). Figure 2(D) shows that the number of expansion clones in the si-FGF5 group (356.00 \pm 16.40) has significantly decreased compared with si-NC (490.67 \pm 48.84) group. Using western bolt assays, protein levels of FGF5 and the indicator of aHSCs, α -SMA were detected after si-FGF5 transfection. It was demonstrated that both FGF5 and α -SMA were obviously decreased in the si-FGF5 group (Figure 2(E)). These results indicated that the suppression of FGF5 impeded the proliferation and expansion of HSCs, subsequently leading to a decrease in the population of activated HSCs.

TABLE 1. Primers for the qRT-PCR

Gene	Primer sequences (5'-3')
FGF5	FGF5(human)-F: GCCTCAGCAATACATAGAAC
	FGF5(human)-R: CAGTAACCGTGAAAGAAAGT
FGF11	FGF11(human)-F: CTCTACAGTTCGCCGATTT
	FGF11(human)-R: GAACGACGCTGGCGGTAG
TGFB1	TGFB1(human)-F: TCAGGTTCTGGCTCAGGTTTA
	TGFB1(human)-R: GCCTCACGGAACCACGAA
TGFB3	TGFB3(human)-F: CAGCAAATTCTCCTTGACAG
	TGFB3(human)-R: TTGCTATCTTGAGTTCGGTGA
hsa-let-7g-5p	hsa-let-7g-5p(human)-F: AACTCCAGCTGGGTGAGGTAGTAGTTTGT
	hsa-let-7g-5p(human)-R: CTCAACTGGTGTCTGGAGTCGGCAATTCAGTTGAGAACTGTAC
GAPDH	GAPDH(Human)-RT-F: GGAGCGAGATCCCTCCAAAAT
	GAPDH(Human)-RT-R: GGCTGTTGTCATACTTCTCATGG
U6	U6-F: CTCGCTTCGGCAGCACA
	U6-R: AACGCTTCACGAATTTGCGT
	URP: TGGTGTCTGGAGTTCG

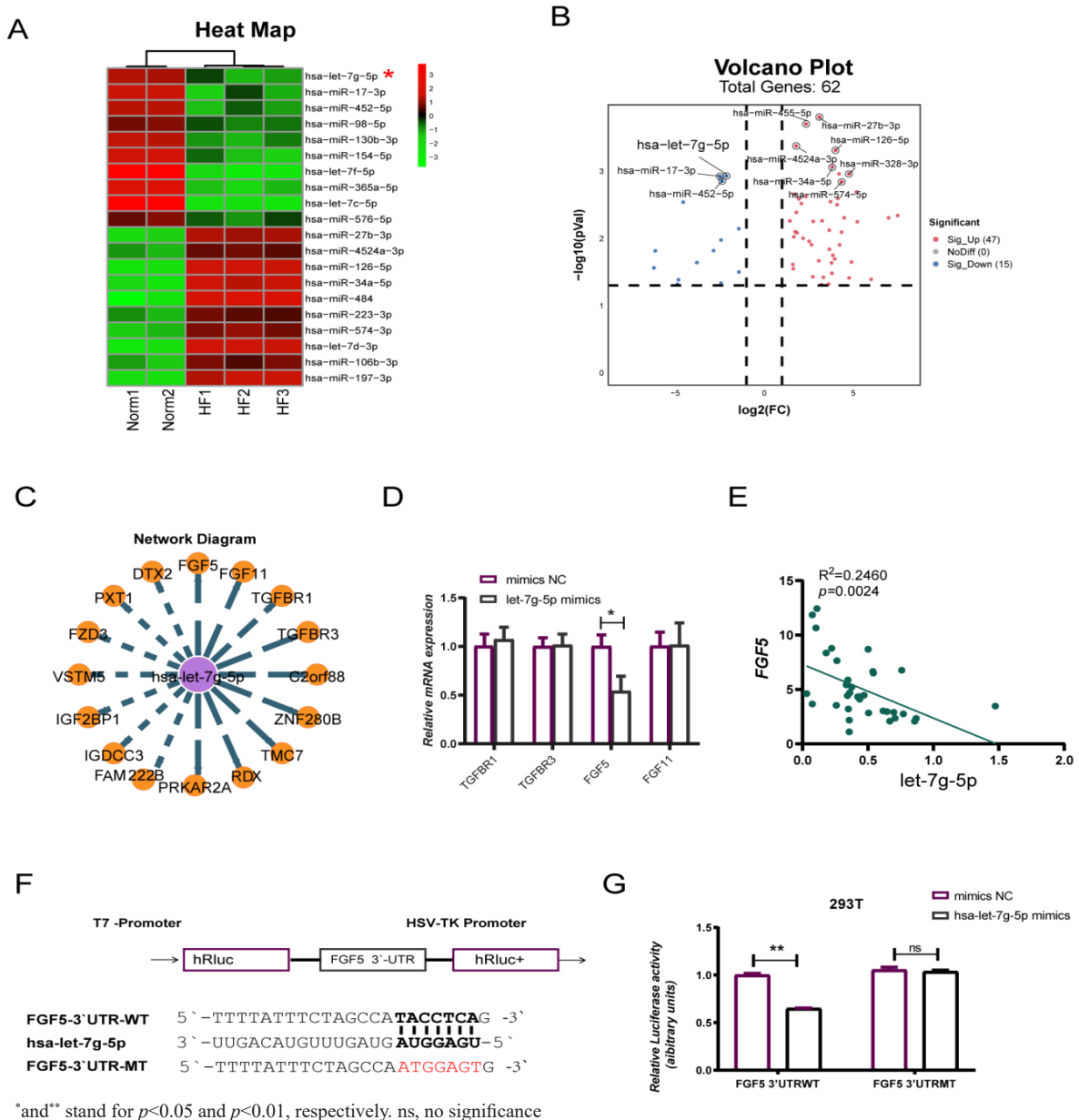
let-7g-5p/FGF5 AXIS SUPPRESSED THE PROLIFERATION
AND EXPANSION OF HSCs, AND DIMINISHED THE
POPULATION OF aHSCs

A rescue assay was designed to further illustrate the role of the let-7g-5p/FGF5 axis in HSCs. Experimental groups include mimics NC (control group); let-7g-5p mimics (experimental group); let-7g-5p mimics+ inhibitor NC (rescue control group); let-7g-5p mimics+ let-7g-5p inhibitor (rescue group).

Firstly, qRT-PCR was performed to detect the mRNA level of FGF5 in each experimental group. As shown in Figure 3(A), FGF5 expression was significantly reduced in the let-7g-5p mimics group compared to the mimics NC group. The experimental group treated with let-7g-5p mimics + let-7g-5p inhibitor exhibited a significant restoration of decreased FGF5

expression. Conversely, the group treated with let-7g-5p mimics + inhibitor NC did not show restoration of FGF5 mRNA expression. The observed recovery was attributed to the competitive binding of the let-7g-5p inhibitor with the let-7g-5p mimics (Figure 3(B)). These results confirmed that let-7g-5p significantly and sensitively downregulated FGF5 expression.

CCK8, EdU, and colony formation assays were assessed for examination of HSCs proliferation and expansion abilities. In the CCK8 assays, the cell proliferation of the let-7g-5p mimics was found to be significantly inhibited ($63.65 \pm 8.09\%$) when compared to the mimics NC group. The proliferation capacity of the group treated with let-7g-5p mimics+let-7g-5p inhibitor was significantly restored ($99.37 \pm 5.56\%$), in comparison to both the group treated with let-7g-5p mimics alone

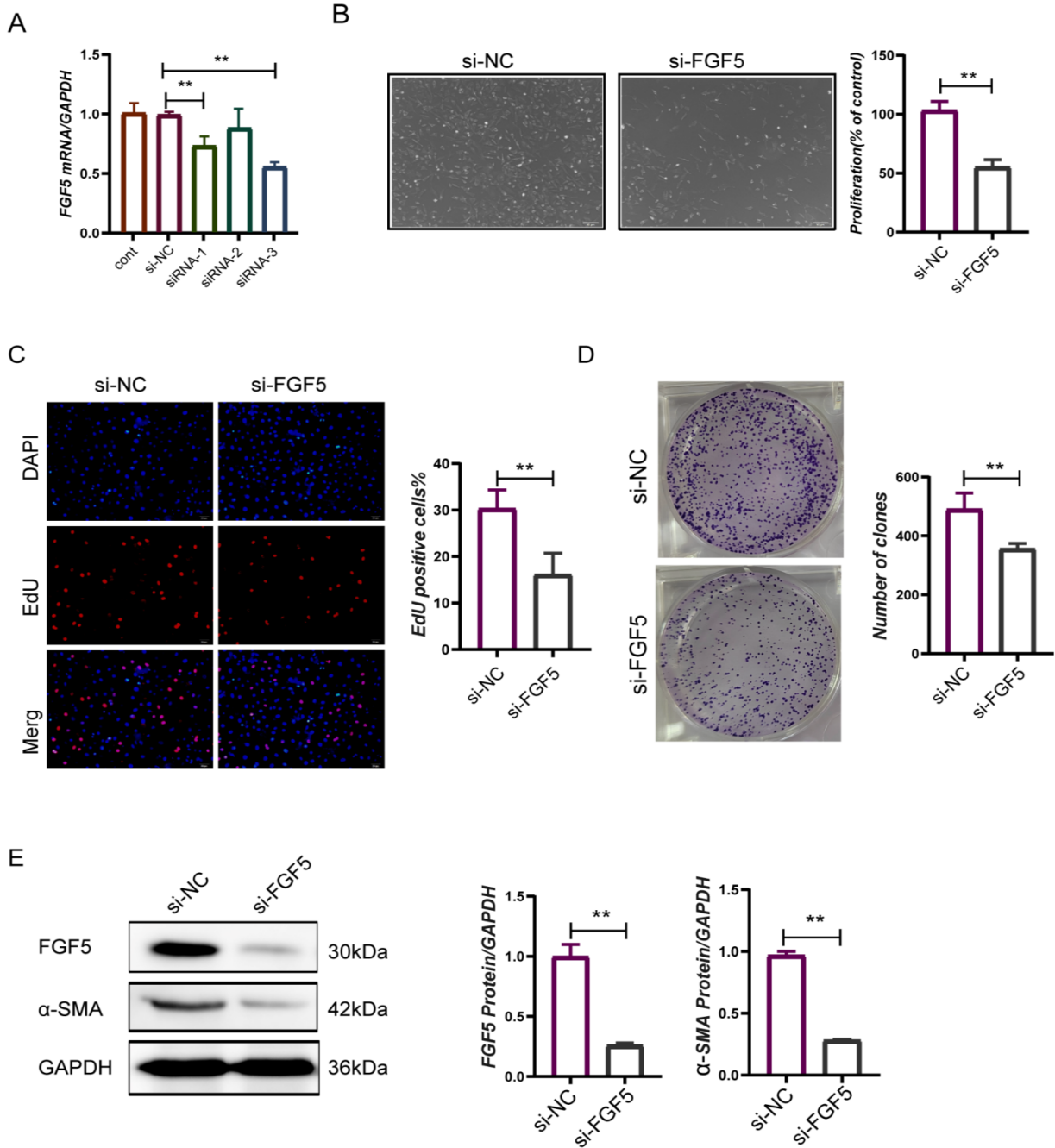


*and** stand for $p < 0.05$ and $p < 0.01$, respectively. ns, no significance

FIGURE 1. let-7g-5p was significantly dysregulated in hepatitis B-related HF samples and directly targeted FGF5 (A) Heat map of the miRNA profile of 3 samples with hepatitis B-related HF. High expression level is indicated by 'red' and lower levels by 'green', (B) miRNA volcano plot. The abscissa is the \log_2 (FC), and the ordinate is $-\log_{10}$ (p -value), (C) Predicted targets of let-7g-5p, (D) qRT-PCR showed FGF5 was significantly downregulated after let-7g-5p mimic transfection, (E) Negative correlation was observed between let-7g-5p and FGF5 in 35 patients with chronic hepatitis B-related HF using qRT-PCR detection, (F) psiCHECK reporter plasmid was used to construct FGF5-3' UTR-WT and FGF5-3' UTR-MT, and (G) Dual-luciferase reporter assay verified the binding relationship between let-7g-5p and FGF5. The RNA levels were normalized to total GAPDH

TABLE 2. Sequencing information of top 15 miRNAs

miR_name	Up/Down	Log2 (FC)	p-values	Abundance	miR_name	p-values
maximal FC					minimal p-values	
(Downregulation)					(Top 15)	
hsa-let-7c-5p	down	-6.20	0.0274	high	hsa-miR-27b-3p (up)	0.0002
hsa-let-7f-5p	down	-6.12	0.0153	high	hsa-miR-4524a-3p (up)	0.0004
hsa-let-7a-5p	down	-4.88	0.0485	high	hsa-miR-126-5p (up)	0.0005
hsa-miR-122-5p	down	-4.88	0.0490	high	hsa-miR-34a-5p (up)	0.0009
hsa-miR-23b-5p	down	-4.82	0.0413	middle	hsa-miR-328-3p (up)	0.0011
hsa-miR-1255b-5p	down	-4.56	0.0029	middle	hsa-let-7g-5p (down)	0.0012
hsa-miR-365a-5p	down	-3.78	0.0229	middle	hsa-miR-17-3p (down)	0.0012
hsa-miR-154-5p	down	-2.85	0.0152	middle	hsa-miR-452-5p(down)	0.0014
hsa-miR-17-3p	down	-2.50	0.0012	middle	hsa-miR-574-5p (up)	0.0014
hsa-miR-29c-3p	down	-2.43	0.0463	middle	hsa-miR-484 (up)	0.0020
hsa-miR-130b-3p	down	-2.42	0.0106	middle	hsa-miR-223-3p (up)	0.0022
hsa-miR-452-5p	down	-2.36	0.0014	middle	hsa-miR-574-3p (up)	0.0024
hsa-let-7g-5p	down	-2.13	0.0012	high	hsa-let-7d-3p (up)	0.0025
hsa-miR-98-5p	down	-1.43	0.0072	middle	hsa-miR-106b-3p (up)	0.0026
hsa-miR-576-5p	down	-1.42	0.0316	middle	hsa-miR-197-3p (up)	0.0028
(Upregulation)						
hsa-miR-126-3p	up	7.50	0.0046	high		
hsa-miR-30b-5p	up	6.99	0.0049	high		
hsa-miR-20a-5p	up	6.01	0.0407	middle		
hsa-miR-374a-5p	up	5.23	0.0057	middle		
hsa-miR-484	up	5.18	0.0020	high		
hsa-miR-194-5p	up	4.90	0.0225	high		
hsa-miR-151a-5p	up	4.77	0.0387	high		
hsa-miR-328-3p	up	4.76	0.0011	middle		
hsa-miR-145-3p	up	4.50	0.0049	middle		
hsa-miR-574-5p	up	4.35	0.0014	middle		
hsa-miR-423-3p	up	4.35	0.0081	high		
hsa-miR-361-3p	up	4.23	0.0125	middle		
hsa-let-7d-3p	up	4.14	0.0025	middle		
hsa-miR-502-3p	up	4.09	0.0032	middle		
hsa-miR-126-5p	up	4.00	0.0005	middle		
hsa-miR-100-5p	up	3.96	0.0202	high		



** stand for $p < 0.01$

FIGURE 2. si-FGF5 inhibited the proliferation and expansion of HSCs and reduced the α -SMA level (A) Optimal siRNA targeting FGF5 was screened by qRT-PCR, (B) The percentage of cell proliferation (% of control) at 48 h after transfection in CCK8 assay, (C) EdU assay. Red indicates EdU staining and blue indicates DAPI (Magnification 100 \times), (D) Colony formation assay, and (E) Protein levels of FGF5 and α -SMA were detected by western blot assay. The RNA and protein levels were normalized to total GAPDH

and the group treated with let-7g-5p mimics + inhibitor NC (67.80±7.23%) (Figure 4(A)). The EdU assay results indicated a significant decrease in the percentage of EdU-positive cells in the let-7g-5p mimics group compared to the mimics NC group. Conversely, the group treated with let-7g-5p mimics + let-7g-5p inhibitor showed an increase in the proportion of EdU-positive cells compared to both the let-7g-5p mimics group and the let-7g-5p mimics+inhibitor NC group (Figure 4(B)). In colony formation assay, let-7g-5p mimics group (388.00±19.92) had an obvious reduction in expansion of clone numbers compared with mimics NC (496.00±35.23). However, there was a significant reversal in the number of clone formations in the group treated with let-7g-5p mimics+ let-7g-5p inhibitor (534.67±33.82) in comparison to both the let-7g-5p mimics group and the let-7g-5p mimics+inhibitor NC group (374.67±21.86) (Figure 4(C)). Next, in each experimental group, FGF5 and α -SMA protein levels were examined. The group treated with let-7g-5p mimics demonstrated a significant decrease in the protein levels of FGF5 and α -SMA. A notable increase of FGF5 and α -SMA expression was observed in the let-7g-5p mimics + let-7g-5p inhibitor group, whereas the let-7g-5p mimics + inhibitor NC group did not demonstrate a significant elevation (Figure 4(D)). These results showed that the let-7g-5p/FGF5 axis significantly inhibited the proliferation and expansion of HSCs. The substantial decrease in α -SMA expression further indicated that this regulatory axis may significantly diminish the population of aHSCs.

let-7g-5p/FGF5 AXIS MITIGATED HF IN BDL MICE

A mouse HF model was constructed by BDL induction (Figure 5(A)). In the BDL/no treatment group, Masson

and VG staining showed significant deposition of collagen fibers in both the portal tract and interstitial region, as compared with the control group. In the BDL/let-7g-5p agomir group, a significant reduction in collagen fiber deposition was observed compared to the BDL/no treatment group. In contrast, the BDL/agomir NC group did not exhibit a substantial decrease in collagen fiber deposition (Figure 5(B) & 5(C)).

Additionally, IHC staining showed that the BDL/no treatment group exhibited a significantly elevated level of FGF5 and α -SMA expression compared to the control group. In the BDL/agomir NC group, the expression levels of FGF5 and α -SMA were comparable to those observed in the BDL/no treatment group. Conversely, the BDL/let-7g-5p agomir group exhibited a significant reduction in the levels of FGF5 and α -SMA (Figure 5(D) & 5(E)). These findings provided confirmation that the let-7g-5p/FGF5 axis exerted a significant inhibitory impact on collagen deposition and α -SMA production *in vivo*.

DISCUSSION

HF is an inevitable pathological process of chronic liver disease towards hepatic cirrhosis or even hepatocellular carcinoma (Dong et al. 2023; Xu et al. 2024). Early intervention of HF is essential to prevent its advancement and enhance patient outcomes. During the initial stage of HF, HSCs undergo activation and subsequently transition into a myofibroblast-like phenotype known as aHSCs. The aHSCs rapidly proliferate and expand and secrete large amounts of collagens. Therefore, effective management of the population of aHSCs is crucial for the inhibition of HF.

miRNAs are a class of non-coding functional small RNA composed of 21~23 nucleotides

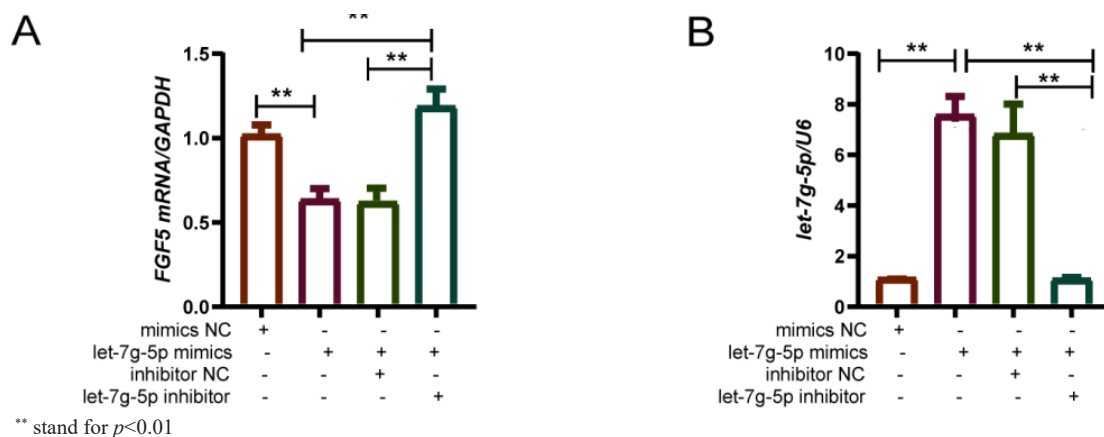
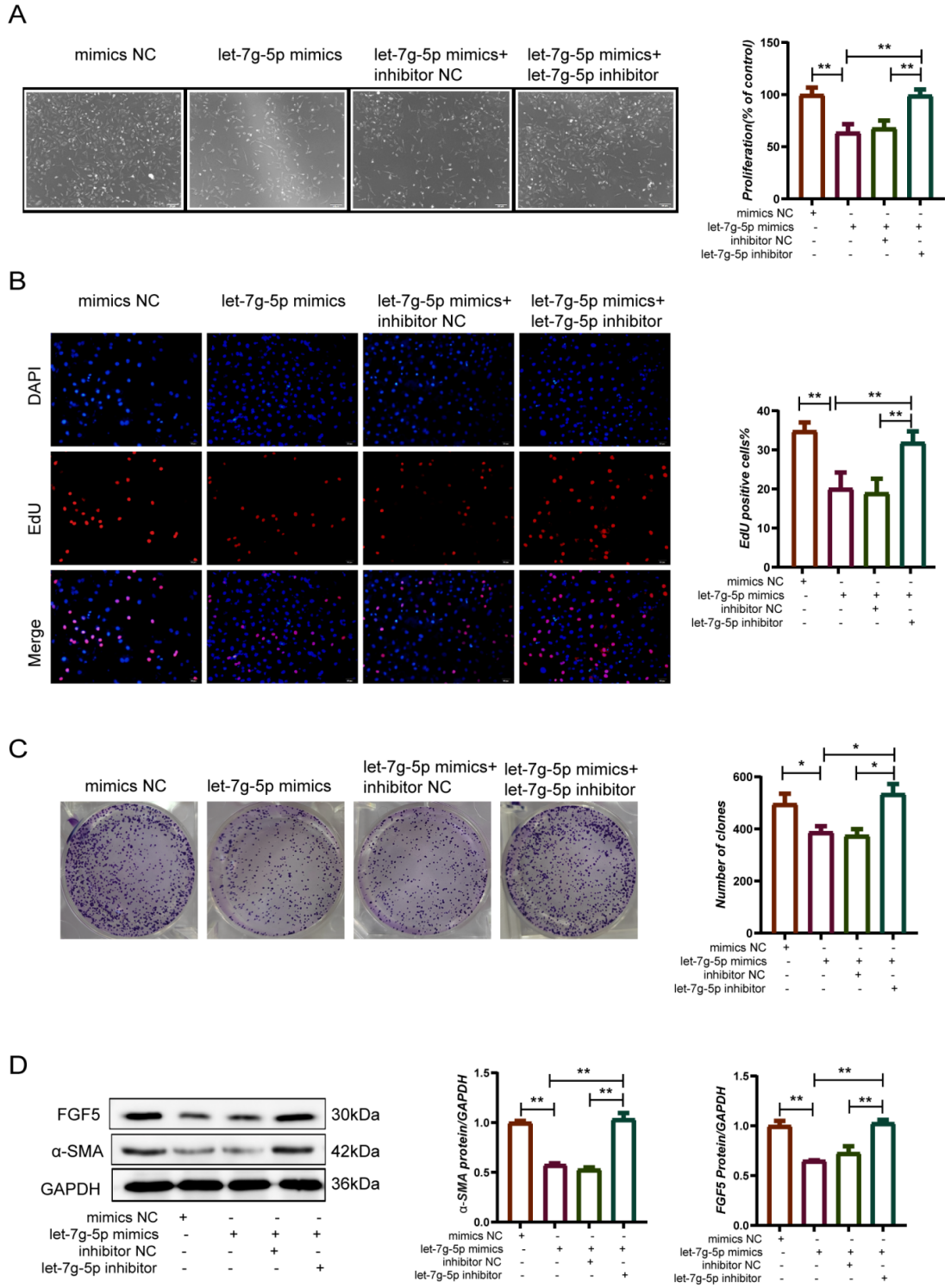
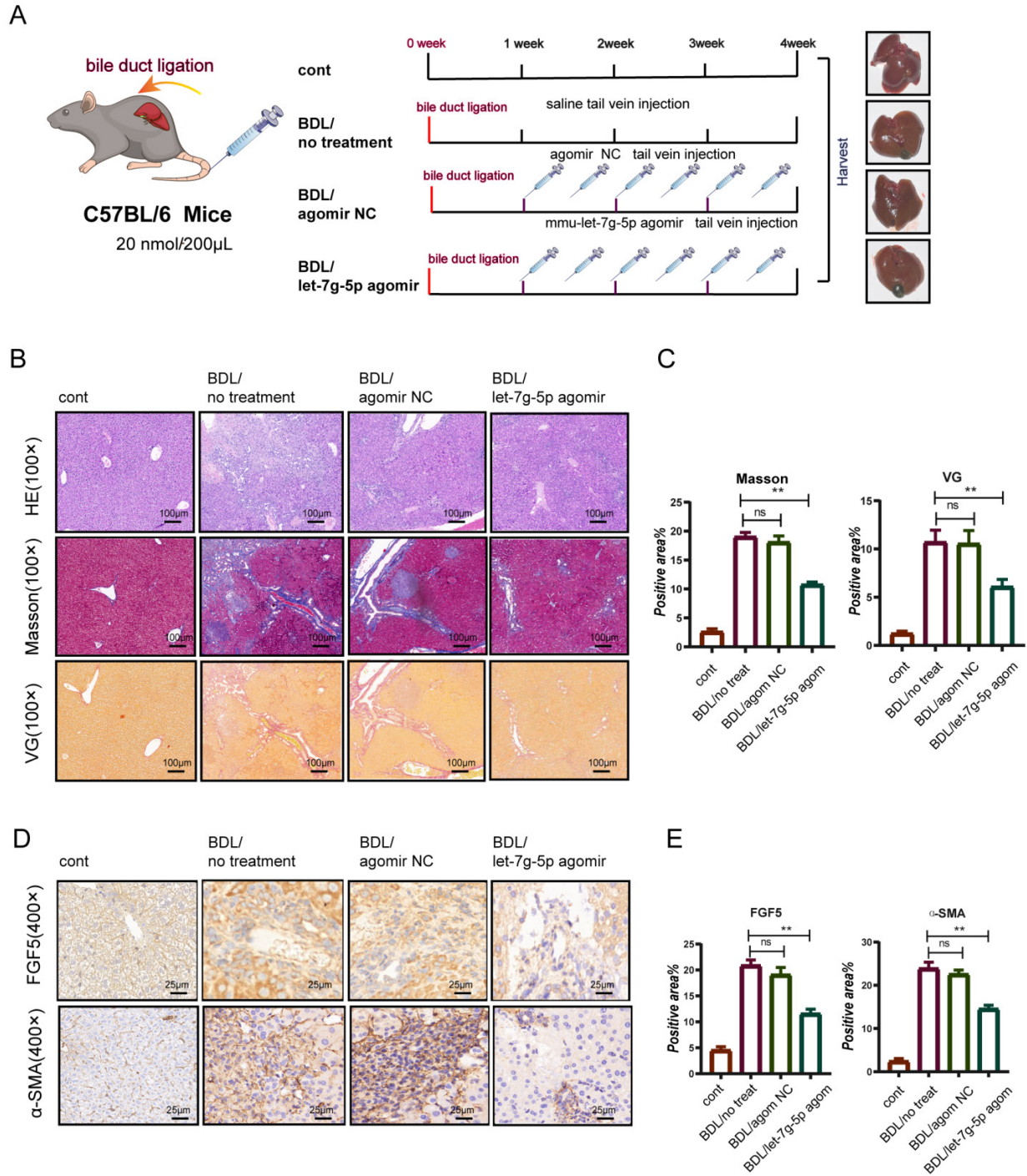


FIGURE 3. let-7g-5p/FGF5 axis was proved through rescue assay in HSCs (A) Expression of FGF5 was significantly reduced in the let-7g-5p mimics group, but restored in the let-7g-5p mimics + let-7g-5p inhibitor group, and (B) let-7g-5p inhibitor competitively binds with let-7g-5p mimics. The mRNA and level were normalized to total GAPDH. The miRNA level was normalized to U6



*and** stand for $p < 0.05$ and $p < 0.01$, respectively

FIGURE 4. let-7g-5p/FGF5 axis suppressed the proliferation and expansion of HSCs and diminished the α -SMA level (A) The percentage of cell proliferation (% of control) at 48 h after transfection in CCK8 assay, (B) EdU assay. Red indicates EdU staining and blue indicates DAPI. (Magnification 100 \times), (C) Colony formation assay, and (D) Protein levels of FGF5 and α -SMA were detected by western blot assay. The mRNA and protein levels were normalized to total GAPDH



** stands for $p < 0.01$. ns, no significance

FIGURE 5. Tail vein injection of mmu-let-7g-5p agomir alleviated collagen deposition and α -SMA production in BDL mice (A) The flow chart of the animal experiment, (B) H&E/Masson/VG/ staining (Magnification 100×; Masson, blue indicates fiber; VG, red indicates fiber), (C) Quantitative analysis for the Masson/VG-positive area, (D) IHC staining (Magnification 400×), and (E) Quantitative analysis for the IHC-positive area

(Goncalves et al. 2023). In general, miRNA targets mRNA via its 3'-UTR, resulting in mRNA degradation or translational repression (Wu et al. 2023). With high biological specificity and low immunogenicity, miRNA has become a promising therapeutic target for diseases (Chioccioli et al. 2022; Li et al. 2023; Rupaimoole & Slack 2017). Recent studies have increasingly proven the significant role of miRNAs in the pathogenesis of organ fibrosis (Yao et al. 2018; Zou et al. 2019). In-depth research to identify the miRNAs with therapeutic potential in HF is warranted. HBV infection is the predominant etiological factor for HF in China. To ensure the generalizability of the research findings, in this study, three hepatitis B-related HF samples were used for RNA-seq. The miRNA profile of human HF was acquired, and among the dysregulated miRNAs, let-7g-5p was focused due to its significant down-regulation and high specificity in the sequencing data (Table 2). The let-7 miRNA family, which is ancient and highly conserved in both vertebrates and invertebrates, consists of 12 different members in humans. let-7 miRNAs are known to play important roles in species evolution, organ development, and the onset of diseases (Lee et al. 2016; Wang et al. 2024; Zhong, Guan & Jin 2022). According to Matsuura et al. (2016), the let-7 levels in plasma show a close correlation with the progression of chronic hepatitis C-related fibrosis in the liver. However, the role of let-7g-5p in hepatitis B-related HF remains unclear.

Our research clarified the function and mechanism of let-7g-5p in HF. FGF5, a member of fibroblast growth factors (FGFs), was identified as the primary target gene downstream of let-7g-5p. A negative correlation was observed between FGF5 and let-7g-5p in thirty-five patients with hepatitis B-related HF. FGFs fulfill crucial roles in cell proliferation, differentiation, and migration (Huang, Liu & Wu 2023). FGF5 was initially identified as a proto-oncogene and exerted potent pro-proliferative effects on non-small cell lung cancer cells and HCC (Fang et al. 2015). In our study, it was demonstrated that the silencing of FGF5 using siRNA significantly impeded the proliferation and expansion of HSCs, and led to an obvious decrease in the level of α -SMA, the marker of aHSCs. It was hypothesized that FGF5 may decrease the number of aHSCs by limiting their amplification. Rescue assay further proved that let-7g-5p significantly hampered the proliferation and expansion of HSCs and reduced the α -SMA expression through targeting FGF5. Additionally, we detected the let-7g-5p/FGF5 regulatory axis in the BDL-induced mice HF models. The injection of let-7g-5p led to a notable decrease of collagens deposition in BDL mice, accompanied by a significant reduction in the levels of FGF5 and α -SMA. Based on these results, it was speculated that let-7g-5p/FGF5 may inhibit HSCs proliferation and expansion, thereby diminishing the population of aHSCs and reducing collagens secretion (Figure 6).

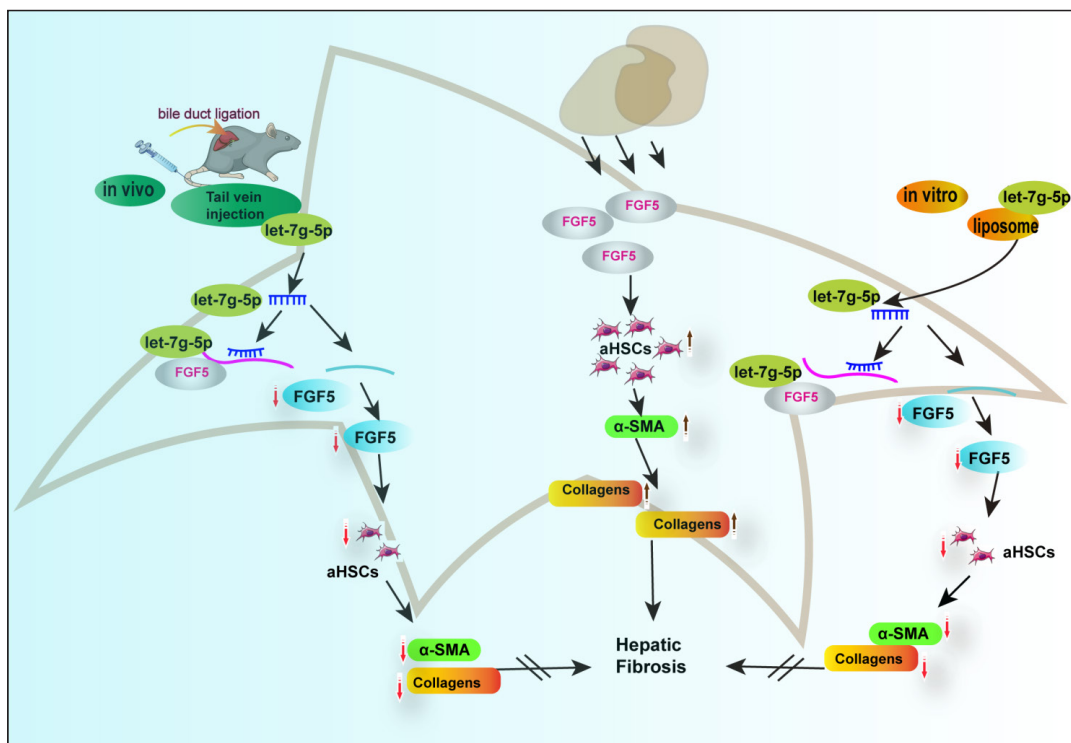


FIGURE 6. Schematic diagram of mechanism of the let-7g-5p/FGF5 axis *in vitro* and *in vivo*

BDL-induced HF represents a persistent injury model leading to progressive liver damage (García et al. 2002). In this model, the let-7g-5p/FGF5 axis exhibited a pronounced inhibitory effect on collagen deposition, indicating its anticipating applicability and clinical translational value. The let-7g-5p/FGF5 axis shows high promise as a novel and viable therapeutic target for the prevention of HF. However, there were also some limitations in the present study. How does this regulatory axis work in other HF animal models (such as CCL₄-induced HF model)? And a larger number of clinical samples should be included to enhance the objectivity of conclusion in this study. We will continue to explore these issues in the follow-up study.

CONCLUSIONS

To summarize, the study identified let-7g-5p as a potential anti-HF regulator through RNA-seq. The research findings indicated that FGF5 functioned as the primary target gene downstream of let-7g-5p. A negative correlation was observed between let-7g-5p and FGF5 in hepatitis B-related HF patients. The let-7g-5p/FGF5 axis was demonstrated to significantly inhibit the proliferation and expansion of HSCs and ameliorate HF in a BDL mice model. The let-7g-5p/FGF5 axis shows promise as a potentially effective therapeutic target for reducing the population of aHSCs in HF.

ACKNOWLEDGMENTS

We express our gratitude to Shanghai Saideng Biotechnology Company for their provision of siRNA design and synthesis services. Jiangsu Province College Students Innovation and Entrepreneurship Training Program (Grant No. 202313993010Y, Grant No. 202313993004Y) supported this research. Author's contributions for this study are as follows, Jiaming Zhou designed the study. Jiaming Zhou, Siyan Huang, Yidan Yang, Yutong Cong, Yuwen Chen and Mengwen Lu carried out the experiment. Jiaming Zhou and Siyan Huang wrote the paper. Jiaming Zhou, Youyou Ding and Meiyuan Li revised the manuscript.

REFERENCES

- Cheng, B., Zhu, Q., Lin, W. & Wang, L. 2019. MicroRNA-122 inhibits epithelial-mesenchymal transition of hepatic stellate cells induced by the TGF- β 1/Smad signaling pathway. *Experimental and Therapeutic Medicine* 17(1): 284-290.
- Chien, Y., Tsai, P.H., Lai, Y.H., Lu, K.H., Liu, C.Y., Lin, H.F., Huang, C.S., Wu, W.W. & Wang, C.Y. 2020. CircularRNA as novel biomarkers in liver diseases. *Journal of the Chinese Medical Association* 83(1): 15-17.
- Chioccioli, M., Roy, S., Newell, R., Pestano, L., Dickinson, B., Rigby, K., Herazo-Maya, J., Jenkins, G., Ian, S., Saini, G., Johnson, S.R., Braybrooke, R., Yu, G., Sauler, M., Ahangari, F., Ding, S., DeJullis, J., Aurelien, N., Montgomery, R.L. & Kaminski, N. 2022. A lung targeted miR-29 mimic as a therapy for pulmonary fibrosis. *EBioMedicine* 85: 104304.
- Dong, J., Zhang, R., Xia, Y., Jiang, X., Zhou, K., Li, J., Guo, M., Cao, X. & Zhang, S. 2023. The necroptosis related gene LGALS3 can be used as a biomarker for the adverse progression from chronic HBV infection to HCC. *Frontiers in Immunology* 14: 1142319.
- Fang, F., Chang, R.M., Yu, L., Lei, X., Xiao, S., Yang, H. & Yang, L.Y. 2015. MicroRNA-188-5p suppresses tumor cell proliferation and metastasis by directly targeting FGF5 in hepatocellular carcinoma. *J. Hepatol.* 63(4): 874-885.
- Friedman, S.L. 2015. Hepatic fibrosis: Emerging therapies. *Digestive Disease* 33(4): 504-507.
- García, L., Hernández, I., Sandoval, A., Salazar, A., García, J., Vera, J., Grijalva, G., Muriel, P., Margolin, S. & Armendariz-Borunda, J. 2002. Pirfenidone effectively reverses experimental liver fibrosis. *Journal of Hepatology* 37(6): 797-805.
- Geerts, A. 2001. History, heterogeneity, developmental biology, and functions of quiescent hepatic stellate cells. *Seminars in Liver Disease* 21(3): 311-335.
- Goncalves, B.S., Meadows, A., Pereira, D.G., Puri, R. & Pillai, S.S. 2023. Insight into the inter-organ crosstalk and prognostic role of liver-derived MicroRNAs in metabolic disease progression. *Biomedicines* 11(6): 1597.
- Ho, J.K., Jeevan-Raj, B. & Netter, H.J. 2020. Hepatitis B virus (HBV) subviral particles as protective vaccines and vaccine platforms. *Viruses* 12(2): 126.
- Huang, Q., Liu, B. & Wu, W. 2023. Biomaterial-based bFGF delivery for nerve repair. *Oxidative Medicine and Cellular Longevity* 2023: 8003821.
- Lee, H., Han, S., Kwon, C.S. & Lee, D. 2016. Biogenesis and regulation of the let-7 miRNAs and their functional implications. *Protein & Cell* 7(2): 100-113.
- Li, H., Liu, T., Yang, Y., Cho, W.C., Flynn, R.J., Harandi, M.F., Song, H., Luo, X. & Zheng, Y. 2023. Interplays of liver fibrosis-associated microRNAs: Molecular mechanisms and implications in diagnosis and therapy. *Genes & Diseases* 10(4): 1457-1469.
- Matsuura, K., De Giorgi, V., Schechterly, C., Wang, R.Y., Farci, P., Tanaka, Y. & Alter, H.J. 2016. Circulating let-7 levels in plasma and extracellular vesicles correlate with hepatic fibrosis progression in chronic hepatitis C. *Hepatology* 64(3): 732-745.
- Pei, Q., Yi, Q. & Tang, L. 2023. Liver fibrosis resolution: From molecular mechanisms to therapeutic opportunities. *International Journal of Molecular Sciences* 24(11): 9671.

- Rupaimoole, R. & Slack, F.J. 2017. MicroRNA therapeutics: Towards a new era for the management of cancer and other diseases. *Nature Reviews Drug Discovery* 16(3): 203-222.
- Thanh Minh Dang, Trinh Van Le, Huy Quang Do, Van Thuan Nguyen, Ai Xuan Le Holterman, Loan Tung Thi Dang, Nhan Chinh Lu Phan, Phuc Van Pham, Son Nghia Hoang, Long Thanh Le, Gabriele Grassi & Nhung Hai Truong. 2021. Optimization of the isolation procedure and culturing conditions for hepatic stellate cells obtained from mouse. *Bioscience Reports* 41(1): BSR20202514.
- Wanless, I.R., Nakashima, E. & Sherman, M. 2000. Regression of human cirrhosis. Morphologic features and the genesis of incomplete septal cirrhosis. *Archives of Pathology & Laboratory Medicine* 124(11): 1599-1607.
- Wang, F., Zhou, C., Zhu, Y. & Keshavarzi, M. 2024. The microRNA Let-7 and its exosomal form: Epigenetic regulators of gynecological cancers. *Cell Biology and Toxicology* 40(1): 42.
- Wang, F., Jia, Y., Li, M., Wang, L., Shao, J., Guo, Q., Tan, S., Ding, H., Chen, A., Zhang, F. & Zheng, S. 2019. Blockade of glycolysis-dependent contraction by oroxylin a via inhibition of lactate dehydrogenase-a in hepatic stellate cells. *Cell Communication and Signaling* 17(1): 11.
- Wang, Q., Wei, S., Zhou, H., Li, L., Zhou, S., Shi, C., Shi, Y., Qiu, J. & Lu, L. 2020. MicroRNA-98 inhibits hepatic stellate cell activation and attenuates liver fibrosis by regulating HLF expression. *Frontiers in Cell and Developmental Biology* 8: 513.
- Wasser, S., Lim, G.Y., Ong, C.N. & Tan, C.E. 2001. Anti-oxidant ebselen causes the resolution of experimentally induced hepatic fibrosis in rats. *Journal of Gastroenterology and Hepatology* 16(11): 1244-1253.
- Wei, R., Wang, J., Wang, X., Xie, G., Wang, Y., Zhang, H., Peng, C-Y., Rajani, C., Kwee, S., Liu, P. & Jia, W. 2018. Clinical prediction of HBV and HCV related hepatic fibrosis using machine learning. *EBioMedicine* 35: 124-132.
- Wu, J., Zhu, Y., Cong, Q. & Xu, Q. 2023. Non-coding RNAs: Role of miRNAs and lncRNAs in the regulation of autophagy in hepatocellular carcinoma (Review). *Oncology Reports* 49(6): 113.
- Xu, X., Feng, J., Wang, X., Zeng, X., Luo, Y., He, X., Yang, M., Lv, T., Feng, Z., Bao, L., Zhao, L., Huang, D. & Huang, Y. 2024. Mitochondrial GRIM19 loss induces liver fibrosis through NLRP3/IL33 activation via reactive oxygen species/NF- κ B signaling. *Journal of Clinical and Translational Hepatology* 12(6): 539-550.
- Xu, T., Pan, L., Li, L., Hu, S., Zhou, H., Yang, C., Yang, J., Li, H., Liu, Y., Meng, X. & Li, J. 2020. MicroRNA-708 modulates hepatic stellate cells activation and enhances extracellular matrix accumulation via direct targeting TMEM88. *Journal of Cellular and Molecular Medicine* 24(13): 7127-7140.
- Yao, W., Li, Y., Han, L., Ji, X., Pan, H., Liu, Y., Yuan, J., Yan, W., Ni, C. 2018. The CDR1as/miR-7/TGFBR2 axis modulates EMT in silica-induced pulmonary fibrosis. *Toxicological Sciences* 166(2): 465-478.
- Zhong, H., Guan, G. & Jin, Y. 2024. Roles of helminth extracellular vesicle-derived let-7 in host-parasite crosstalk. *Frontiers in Immunology* 15: 1449495.
- Zou, Y., Li, S., Li, Z., Song, D., Zhang, S. & Yao, Q. 2019. MiR-146a attenuates liver fibrosis by inhibiting transforming growth factor- β 1 mediated epithelial-mesenchymal transition in hepatocytes. *Cellular Signaling* 58: 1-8.

*Corresponding author; email: zhoujiaming@ntu.edu.cn

TABLE 1. Primers for the qRT-PCR

Gene	Primer sequences (5`-3`)
FGF5	FGF5(human)-F: GCCTCAGCAATACATAGAAC FGF5(human)-R: CAGTAACCGTGAAAGAAAGT
FGF11	FGF11(human)-F: CTCTACAGTTCGCCGCATT FGF11(human)-R: GAACGACGCTGGCGGTAG
TGFBR1	TGFBR1(human)-F: TCAGGTTCTGGCTCAGGTTTA TGFBR1(human)-R: GCCTCACGGAACCACGAA
TGFBR3	TGFBR3(human)-F: CAGCAAACCTCTCCTTGACAG TGFBR3(human)-R: TTGCTATCTTGAGTTCGGTGA
hsa-let-7g-5p	hsa-let-7g-5p(human)-F: ACACTCCAGCTGGGTGAGGTAGTAGTTTGT hsa-let-7g-5p(human)-R: CTCAACTGGTGTTCGTGGAGTCGGCAATTCAGTTGAGAACTGTAC
GAPDH	GAPDH(Human)-RT-F: GGAGCGAGATCCCTCCAAAAT GAPDH(Human)-RT-R: GGCTGTTGTCATACTTCTCATGG
U6	U6-F: CTCGCTTCGGCAGCACA U6-R: AACGCTTCACGAATTTGCGT URP: TGGTGTTCGTGGAGTCG

TABLE 2. Sequencing information of top 15 miRNAs

miR_name	Up/ Down	Log2 (FC)	p-values	Abundance	miR_name	p-values
maximal FC					minimal p-values	
(Downregulation)					(Top 15)	
hsa-let-7c-5p	down	-6.20	0.0274	high	hsa-miR-27b-3p (up)	0.0002
hsa-let-7f-5p	down	-6.12	0.0153	high	hsa-miR-4524a-3p (up)	0.0004
hsa-let-7a-5p	down	-4.88	0.0485	high	hsa-miR-126-5p (up)	0.0005
hsa-miR-122-5p	down	-4.88	0.0490	high	hsa-miR-34a-5p (up)	0.0009
hsa-miR-23b-5p	down	-4.82	0.0413	middle	hsa-miR-328-3p (up)	0.0011
hsa-miR-1255b-5p	down	-4.56	0.0029	middle	hsa-let-7g-5p (down)	0.0012
hsa-miR-365a-5p	down	-3.78	0.0229	middle	hsa-miR-17-3p (down)	0.0012
hsa-miR-154-5p	down	-2.85	0.0152	middle	hsa-miR-452-5p (down)	0.0014
hsa-miR-17-3p	down	-2.50	0.0012	middle	hsa-miR-574-5p (up)	0.0014
hsa-miR-29c-3p	down	-2.43	0.0463	middle	hsa-miR-484 (up)	0.0020
hsa-miR-130b-3p	down	-2.42	0.0106	middle	hsa-miR-223-3p (up)	0.0022
hsa-miR-452-5p	down	-2.36	0.0014	middle	hsa-miR-574-3p (up)	0.0024
hsa-let-7g-5p	down	-2.13	0.0012	high	hsa-let-7d-3p (up)	0.0025
hsa-miR-98-5p	down	-1.43	0.0072	middle	hsa-miR-106b-3p (up)	0.0026
hsa-miR-576-5p	down	-1.42	0.0316	middle	hsa-miR-197-3p (up)	0.0028
(Upregulation)						
hsa-miR-126-3p	up	7.50	0.0046	high		
hsa-miR-30b-5p	up	6.99	0.0049	high		
hsa-miR-20a-5p	up	6.01	0.0407	middle		
hsa-miR-374a-5p	up	5.23	0.0057	middle		
hsa-miR-484	up	5.18	0.0020	high		
hsa-miR-194-5p	up	4.90	0.0225	high		
hsa-miR-151a-5p	up	4.77	0.0387	high		
hsa-miR-328-3p	up	4.76	0.0011	middle		
hsa-miR-145-3p	up	4.50	0.0049	middle		
hsa-miR-574-5p	up	4.35	0.0014	middle		
hsa-miR-423-3p	up	4.35	0.0081	high		
hsa-miR-361-3p	up	4.23	0.0125	middle		
hsa-let-7d-3p	up	4.14	0.0025	middle		
hsa-miR-502-3p	up	4.09	0.0032	middle		
hsa-miR-126-5p	up	4.00	0.0005	middle		
hsa-miR-100-5p	up	3.96	0.0202	high		

Supplemental Table 1. Sequence analysis

Index	miR_name	miR_seq	up/down	fold_change(Group/Normal)	log2(fold_change)	pvalue(t_test)	Normal (mean)	Group (mean)	Group/C10 (norm)	Group/C11 (norm)	Group/C12 (norm)	Normal/ N2(norm)	Normal/ N1(norm)	Group/C10 (raw)	Group/C11 (raw)	Group/C12 (raw)	Normal/N1 (raw)	Normal/N2 (raw)	Expression level (raw)	
2	hsamiR-27b-3p	TTCAAGTGGCTAGTCTCTCC	up	8.55	3.10	0.0002	3401	29095	27.561	29.103	30.619	2.822	3.981	34.673	70.670	35.527	681	888	high	
5	hsamiR-424a-3p	TGAGACAGGCTTAGCTGCTAT	up	3.47	1.79	0.0004	34	119	12.6	11.3	11.8	37	31	156	275	137	9	7	middle	
8	hsamiR-126-3p	CATTATACCTTTGGTACCGC	up	16.05	4.00	0.0005	186	2,980	3,057	2,837	3,045	174	197	3,779	6,890	3,533	42	44	middle	
12	hsamiR-34b-5p	TGGCAGTGTCTTAGTGGTGT	up	14.08	3.82	0.0009	75	1,052	960	1,093	1,104	91	58	1,187	2,054	1,281	22	13	high	
15	hsamiR-328-3p	CTGGCCCTCTCCCTCCCT	up	27.11	4.76	0.0011	13	365	381	394	319	0	27	471	956	370	0	6	middle	
17	hsamiR-7g-5p	TGAGGTAGTAGTTGTACAGTT	down	0.23	-2.13	0.0012	136,640	31,287	23,144	26,715	44,002	139,566	892	856	292	327	109	215	191	high
18	hsamiR-17-3p	ACTCGACGAGGACACTGTAG	down	0.18	-2.50	0.0012	874	155	23.6	135	94	48	336	332	108	145	56	81	74	middle
20	hsamiR-452-5p	AACCTTTGAGAGGAAGCTGA	down	0.20	-2.36	0.0014	334	65	87	60	48	29	0	391	745	311	7	0	middle	
21	hsamiR-574-5p	TGAGTGTGTGTGTAGTGTGT	up	20.45	4.35	0.0014	79	2,857	3,092	2,892	2,588	50	108	3,822	7,023	3,003	12	24	high	
26	hsamiR-484	TCAGGCTCAGTCCCTCCCGAT	up	36.32	5.18	0.0020	227	733	701	683	815	257	197	866	1,658	946	62	44	middle	
27	hsamiR-223-3p	TGTGATGTTGTCAAAATACCCA	up	3.23	1.69	0.0022	227	733	701	683	815	257	197	866	1,658	946	62	44	middle	
29	hsamiR-574-3p	CACGCTCATGAGAGCCACA	up	5.08	2.35	0.0024	908	4,614	5,124	4,301	4,418	821	995	6,335	10,444	5,126	198	222	high	
33	hsamiR-7d-3p	CTATAGACCTGGTCCCTTCT	up	17.65	4.14	0.0025	93	1,642	1,591	1,530	1,804	83	103	1,967	3,715	2,093	20	23	middle	
34	hsamiR-106b-3p	CCGACTGTGGGTACTGTGTC	up	3.88	1.96	0.0026	139	540	471	574	577	158	121	582	1,394	669	38	27	middle	
36	hsamiR-197-3p	TTACCCAGCTTCTCCACCAGC	up	13.23	3.73	0.0028	157	2,078	2,169	2,193	1,871	162	152	2,681	5,236	2,171	39	34	middle	
38	hsamiR-125b-5p	CGGATGAGCAAGAAGTGTGT	down	0.04	-4.56	0.0029	24	1	0	0	3	25	22	0	0	4	6	5	middle	
39	hsamiR-188b-3p	TCAGTGCATCAGAGACTTGT	up	4.25	2.09	0.0030	559	2,378	2,534	2,479	2,321	634	484	2,886	6,020	2,693	153	108	high	
40	hsamiR-502-3p	AATGCACCTGGGAAAGATCA	up	17.08	4.09	0.0032	19	319	324	365	267	37	0	401	887	310	9	0	middle	
50	hsamiR-188a-3p	TCAGTGCATCAGAGACTTGT	up	3.50	1.81	0.0041	14,587	51,025	49,397	45,461	58,218	16,646	12,529	61,067	110,391	67,549	4,014	2,795	high	
54	hsamiR-126-3p	TCGTACCTGTAGTAATAATCG	up	180.78	7.50	0.0046	160	28,841	29,364	25,215	31,943	211	108	36,301	61,229	37,063	51	24	high	
60	hsamiR-143-3p	GGATCTCGAAMACTGTTCT	up	22.55	4.50	0.0049	15	327	290	392	299	29	0	359	953	347	7	0	middle	
66	hsamiR-125b-5p	TCCTTAGACCTTAAGTCTTGA	up	9.50	3.25	0.0055	53,326	50,603	49,550	45,340	56,919	5,459	5,193	61,257	110,099	66,042	1,317	1,159	high	
67	hsamiR-28c-3p	CACATAGATGGTCCCTCGGA	up	2.72	1.44	0.0055	474	1,286	1,377	1,172	1,309	539	408	1,702	2,845	1,519	130	91	middle	
70	hsamiR-193b-3p	AACCTGGCTCAAGTCCCGCT	up	6.72	2.75	0.0056	1,614	10,856	12,675	9,445	10,448	813	2,416	15,670	22,934	12,122	196	539	high	
72	hsamiR-374a-5p	TTATATCAAACTGTAAATG	up	37.59	5.23	0.0057	33	1,238	1,107	1,175	1,433	17	49	1,369	2,854	1,663	4	11	middle	
84	hsamiR-98-5p	TGAGGTAGTAGTGTGTGT	down	0.37	-1.43	0.0072	1,482	549	484	536	628	1,420	1,543	599	1,301	728	342	344	middle	
85	hsamiR-425-5p	AATGACAGCACTCCCTGTGA	up	12.58	3.65	0.0076	98	1,121	1,420	1,033	1,239	75	121	1,755	2,509	1,438	18	27	middle	
90	hsamiR-92b-3p	TATTCACCTTCCCGCCCTGT	up	3.33	1.74	0.0080	9,476	31,549	35,153	25,794	33,700	7,877	11,074	43,458	62,635	39,101	1,900	2,471	high	
91	hsamiR-423-3p	AGCTGGCTGTGAGGCCCTCATG	up	20.33	4.35	0.0081	479	9,743	8,349	9,559	11,221	564	394	10,322	23,212	13,136	136	88	high	

continue to next page

continue from previous page

92	basemR-92-5p	CAAAATGCTGTTGTCAGAGTAG	3.58	1.84	0.0083	551	1,974	2,301	1,644	1,978	448	654	2,845	3,391	2,295	108	146	middle
102	basemR-409-3p	GAATGTTGCTGGTGAACCCCT	3.17	1.66	0.0095	30	96	78	106	105	25	36	96	257	122	6	8	middle
107	basemR-996-5p	CACCCGTAGACCGACCTTCGG	4.54	2.18	0.0100	2438	11,074	8,972	13,247	11,003	3,110	1,766	11,092	32,167	12,766	750	394	high
111	basemR-130b-3p	CAGTGAATGATGAAGGEGCAT	0.19	-2.42	0.0106	490	91	75	107	91	510	471	93	261	106	123	105	middle
117	basemR-365b-3p	TATGCCCTCAAAATCCCTAT	5.76	2.53	0.0110	497	2,859	3,475	2,825	2,277	326	668	4,296	6,861	2,643	79	149	middle
124	basemR-186-5p	CAAGAATTCCTCTTGCGCT	6.31	2.66	0.0125	157	993	1,031	1,135	814	153	161	1,274	2,755	944	37	36	middle
125	basemR-361-3p	TCCCCAGGTGTGATCTGATTT	18.80	4.23	0.0125	26	488	464	589	412	23	29	574	1,431	478	6	7	middle
132	basemR-160a-5p	TGAGAACTGAATCCATGGGTT	12.61	3.66	0.0145	216	2,724	2,006	3,340	2,824	369	63	2,480	8,112	3,277	89	14	middle
136	basemR-154-5p	TAGGTATCCGTGTCCTCCG	0.14	-2.85	0.0152	89	12	11	8	18	83	94	13	20	21	20	21	middle
137	baslet-76-5p	TGAGGTAGTAGTGTATAGTT	0.01	-6.12	0.0153	1,385,574	19,906	15,363	17,306	27,051	###	###	18,892	42,023	31,386	342,598	301,261	high
164	basemR-190-3p	TGTCAAAATCCAGAAACTGA	14.49	3.86	0.0178	123	1,784	1,375	1,731	2,245	60	186	1,700	4,203	2,605	15	42	middle
172	basemR-100-5p	AACCCGTAGTCCGACTGTG	15.59	3.96	0.0225	2,695	42,016	31,680	43,119	51,249	2,789	2,602	39,165	104,703	59,464	673	581	high
177	basemR-766-3p	ACTCCAGCCCAAGCCCTCAGC	8.37	3.07	0.0215	16	131	96	168	129	0	31	119	409	150	0	7	middle
181	basemR-194-5p	TGTAAAGCAACTCCATGTGGA	29.96	4.90	0.0225	627	18,795	16,371	15,654	24,358	475	780	20,239	38,013	28,263	115	174	high
185	basemR-365a-5p	AGGGAGCTTTGGGGCAGATGG	0.07	-3.78	0.0229	404	29	21	34	33	386	421	26	83	38	93	94	middle
187	basemR-17-5p	CAAAATGCTACAGTCCAGTAG	13.77	3.78	0.0232	211	2,905	2,677	2,248	3,789	104	318	3,309	5,460	4,396	25	71	middle
196	basemR-22-3p	AAGCTCCAGTTGAAGACTGT	3.05	1.61	0.0245	6,776	20,685	25,586	18,046	18,444	6,187	7,365	31,606	43,821	21,400	1,492	1,643	high
213	baslet-76-5p	TGAGGTAGTAGTGTATAGTT	0.01	-6.20	0.0274	5,501,822	7,480	8,133	6,707	7,601	573,570	526,734	10,084	16,287	8,820	138,313	117,507	high
220	basemR-363-3p	AATGACGGTATCCATCTGA	3.10	1.63	0.0282	50	155	163	114	187	41	58	201	277	217	10	13	middle
233	basemR-576-5p	ATTCATTTCCAGCTCTT	0.37	-1.42	0.0316	54	20	15	23	22	50	58	19	57	25	12	13	middle
243	basemR-542-3p	TGTGACGATGTGATCTGAAA	13.95	3.80	0.0330	12	174	137	141	243	25	0	169	342	282	6	0	middle
262	basemR-504-5p	AGAACCTGGTCTGCATCTATC	6.63	2.73	0.0372	27	179	128	236	172	54	0	158	572	200	13	0	middle
265	basemR-885-5p	TCCATACACTCCCTGCTCT	10.01	3.32	0.0379	302	3,018	4,095	2,343	2,616	301	303	5,063	5,690	3,015	73	68	middle
272	basemR-151a-5p	TCGAGAGCTCAGACTAGT	27.31	4.77	0.0387	235	6,426	4,739	5,659	8,881	251	220	5,859	13,743	10,304	61	49	high
278	basemR-20b-5p	TAAAGTCTATGTCGAGTAG	64.33	6.01	0.0407	97	6,215	5,107	4,779	8,759	50	143	6,313	11,694	10,163	12	32	middle
287	basemR-23b-5p	TGGGTTCTCGCATCTGATTT	0.04	-4.82	0.0413	3,898	138	97	143	174	3,645	4,151	120	347	202	879	926	middle
303	basemR-20c-3p	TAGGACCATTTGAATCCGTTA	0.19	-2.43	0.0463	7,162	1,369	1,499	1,236	1,373	7,846	6,879	1,853	3,001	1,593	1,892	1,535	middle
306	basemR-199a-5p	CCCAGGTTCCAGACTCTGTC	12.28	3.62	0.0479	371	4,550	5,077	5,929	2,644	533	208	6,277	14,398	3,068	129	47	high
307	baslet-7a-5p	TGAGGTAGTAGTGTATAGTT	0.03	-4.88	0.0485	843,011	26,558	26,588	28,031	31,056	905,307	780,715	32,869	68,067	36,033	218,309	174,166	high
308	basemR-362-5p	AATCTCGAACCATGTTGGTAGT	9.30	3.22	0.0486	17	154	142	163	157	33	0	176	397	182	8	0	middle
310	basemR-122-5p	TGGAGTGTGACATGGTGTG	0.03	-4.88	0.0490	24,404,314	###	665,580	614,121	1,214,255	###	###	822,825	1,491,246	1,408,873	5,427,704	5,867,240	high
3	basemR-485-5p	TATGTGCTTTGGACTGATCC	5.10	2.35	1.0000	125	640	632	676	613	112	139	781	1,642	711	27	31	middle